This research was originally published in JNM . Altai M, Wållberg H, Honarvar H, Strand J, Orlova A, Varasteh Z, Sandström M, Löfblom J, Larsson E, Strand SE, Lubberink M, Ståhl S, Tolmachev V. 188Re-ZHER2:V2, a Promising Affibody-Based Targeting Agent Against HER2-Expressing Tumors: Preclinical Assessment. J Nucl Med. 2014;55:1842-8.
http://jnm.snmjournals.org/content/55/11/1842.long

^{188}Re-$Z_{HER2:V2}$, a promising affibody-based targeting agent against HER2-expressing tumors: preclinical assessment.

Mohamed Altai[1], Helena Wållberg[2], Hadis Honarvar[1], Joanna Strand[1] , Anna Orlova[3], Zohreh Varasteh[3], Mattias Sandström[4,5], John Löfblom[2], Erik Larsson[6], Sven-Erik Strand[6], Mark Lubberink [4,5], Stefan Ståhl[2], Vladimir Tolmachev[1].

[1] Division of Biomedical Radiation Sciences, Uppsala University, Uppsala, Sweden;
[2] KTH Royal Institute of Technology, School of Biotechnology, Division of Protein Technology, Stockholm, Sweden;
[3] Preclinical PET Platform, Department of Medicinal Chemistry, Uppsala University, Uppsala, Sweden;
[4] Nuclear medicine and PET, Uppsala University, Uppsala, Sweden;
[5] Medical physics, Uppsala University Hospital, Uppsala, Sweden;
[6] Medical Radiation Physics, Clinical Sciences, Lund University, Lund, Sweden.

This research was supported in part by grants from the Swedish Cancer Society (Cancerfonden), Swedish Research Council (Vetenskapsrådet) and Governmental Funding of Clinical Research within the National Health Service (ALF).

Corresponding author: Vladimir Tolmachev, Professor.

Biomedical Radiation Sciences, Uppsala University, Se- 75185, Uppsala; Sweden

Tel. +46184713414; Fax. +46184713432; E-mail vladimir.tolmachev@bms.uu.se

First author: Mohamed Altai, PhD student,

Biomedical Radiation Sciences, Uppsala University, Se- 75185, Uppsala; Sweden

Tel. +46184713414; Fax. +46184713868; E-mail mohamed.altai@bms.uu.se

ABSTRACT

Affibody molecules are small (7 kDa) non-immunoglobulin scaffold proteins with favorable tumor targeting properties. Studies concerning influence of chelators on biodistribution of ^{99m}Tc-labelled affibody molecules demonstrated that the variant with a C-terminal glycyl-glycyl-glycyl-cysteine peptide-based chelator (designated $Z_{HER2:V2}$) has the best biodistribution profile in vivo and the lowest renal retention of radioactivity. The aim of this study was to evaluate ^{188}Re-$Z_{HER2:V2}$ as a potential candidate for radionuclide therapy of HER2-expressing tumors.

Methods. $Z_{HER2:V2}$ was labelled with ^{188}Re using a gluconate-containing kit. Targeting of HER2-overexpressing SKOV-3 ovarian carcinoma xenografts in nude mice was studied for a dosimetry assessment.

Results. Binding of ^{188}Re-$Z_{HER2:V2}$ to living SKOV-3 cells was demonstrated to be specific with an affinity of 6.4±0.4 pM. The biodistribution study showed a rapid blood clearance (1.4±0.1 %IA/g at 1h p.i.). The tumor uptake was 14±2, 12±2, 5±2 and 1.8±0.5 %IA/g at 1, 4, 24 and 48 h p.i., respectively. The in vivo targeting of HER2 expressing xenografts was specific. Already at 4 h p.i, the tumor uptake exceeded uptake in kidneys (2.1±0.2 %IA/g). Scintillation-camera imaging showed that tumor xenografts were the only sites with prominent accumulation of radioactivity at 4h p.i. Based on the biokinetics, a dosimetry evaluation for humans suggests that ^{188}Re-$Z_{HER2:V2}$ would provide an absorbed dose to tumour of 79 Gy without exceeding absorbed doses of 23 Gy to kidneys and 2 Gy to bone marrow. This indicates that future human radiotherapy studies may be feasible.

Conclusion. ^{188}Re-$Z_{HER2:V2}$ can deliver high absorbed doses to tumors without exceeding kidney and bone marrow toxicity limits.

KEYWORDS

HER2, Affibody molecule, Rhenium-188, Dosimetry.

INTRODUCTION

Overexpression of the human epidermal growth factor receptor type-2 (HER2) is associated with malignant transformation of cells and provides a growth advantage for tumors. Treatment of HER2-expressing disseminated tumors with the anti-HER2 monoclonal antibody trastuzumab improves survival of patients with metastatic breast (*1*) and gastric cancer (2). However, many tumors have a primary trastuzumab resistance or develop resistance during therapy despite preserved HER2 expression (*2*). Conjugation of cytotoxic payloads (e.g. drugs or radionuclides) to tumor-targeting antibodies may enhance their anti-tumor effects and hence improve the response duration and overall response rate (*3,4*). Beta-emitting radionuclides are considered as a promising form of cytotoxic payload, because of the cross-fire effect. The use of full-length antibodies for radionuclide therapy, however, is associated with a number of issues. The major obstacles are insufficient penetration in the tumor tissue, limiting the absorbed dose to tumors and slow clearance from the body causing second organ (mainly bone marrow) toxicity (*5*). The use of smaller targeting agents, e.g. antibody fragments, would provide more efficient extravasation, better tumor penetration and more rapid clearance of an unbound tracer (*6,7*).

A promising approach for development of high affinity small-size tumor targeting agents is the use of engineered scaffold proteins (*8*). Affibody molecules are the most studied class of scaffold proteins for in vivo radionuclide targeting. These high affinity ligands are based on a 58 amino acid (7 kDa) triple alpha-helical scaffold derived from domain B of staphylococcal protein A (*9*). An affibody with picomolar affinity (22 pM) to the extracellular domain of HER2 has been selected earlier (*10*). Affibody molecules labelled with different radionuclides have demonstrated efficient tumor targeting and high-contrast imaging of HER2-expressing tumors (11). Two clinical studies have demonstrated that affibody molecules are non-toxic and non-immunogenic in humans (*12,13*). However, affibody molecules undergo renal

excretion followed by efficient substantial renal re-absorption (*14*). The use of residualizing labels has therefore resulted in a high retention of radionuclides in kidneys with a radioactivity concentration exceeding several fold the radioactivity concentration in tumors. This would make the use of majority of radiometals (e.g. ^{177}Lu or ^{90}Y) unsuitable for radionuclide therapy (*11*). An important feature of the HER2-targeting affibody molecules is their slow internalization by HER2-expressing cells (*15*). This enables the use of non-residualizing labels without appreciable reduction of tumor retention. On the contrary, rapid internalization of the affibody in proximal tubuli results in rapid clearance of non-residualizing labels from kidneys (*11,16*).

Earlier, we have evaluated how the composition of peptide-based N_3S chelators can influence the targeting and biodistribution properties of ^{99m}Tc-labelled affibody molecules. Mercaptoacetyl-containing chelators on N-terminus (*17-20*) and cysteine-containing chelators on C-terminus (*21-23*) were evaluated. We have shown that biodistribution of affibody molecules can be altered by varying the amino acid composition of such chelators. Importantly, residualizing properties of ^{99m}Tc-label can be modulated in a wide range. For example, ^{99m}Tc-$Z_{HER2:V2}$ variant having a -GGGC peptide chelator at the C-terminus demonstrated tumor uptake exceeding its renal uptake appreciably due to weak residualizing properties (*22*).

Rhenium is a chemical analogue to technetium. The beta-emitting rhenium isotope ^{188}Re (T½=17.0 h; E_{β^-} max=2.1 MeV) has a potential for therapeutic applications. Production via a generator with a long-lived mother nuclide ^{188}W (T½=70 d) makes this radionuclide readily available with high specific radioactivity. A low-abundance (15%) low-energy (155 keV) gamma emission enables imaging of biodistribution of ^{188}Re-labeled therapeutic agents in

patients for patient-specific dosimetry. We expected that substitution of ^{99m}Tc for ^{188}Re in affibody molecules might provide a conjugate with a high tumor uptake and low renal retention. However, the chemical properties of rhenium and technetium are similar but not identical and biodistribution of ^{99m}Tc- and ^{188}Re-labelled peptides can be different (*24*,*25*). Therefore, an evaluation of ^{188}Re-labelled $Z_{HER2:V2}$ was necessary.

The goal of the current study was to evaluate the tumor-targeting properties and biokinetics of ^{188}Re-$Z_{HER2:V2}$ in mice bearing HER2-expressing xenografts and based on dosimetry evaluation determine whether ^{188}Re-$Z_{HER2:V2}$ might be a candidate for treatment of HER2-expressing tumors without severe second organ toxicity.

MATERIALS AND METHODS

^{188}Re was obtained as perrhenate by elution of a ^{188}W/^{188}Re generator (29.6 GBq) with 0.9% sodium chloride (Polatom). Affibody molecule $Z_{HER2:V2}$ was produced and purified as described by (*26*). All chemicals were purchased from Sigma-Aldrich. The HER2-expressing ovarian cancer cell line SKOV-3, $1.6x10^6$ HER2 receptors per cell (ATCC), was used in cell studies. Cells were cultured in RPMI medium supplemented with 10% fetal calf serum, 2 mM L-glutamine and PEST (penicillin 100 IU/ml and 100 μg/ml streptomycin).

Labelling and Stability

$Z_{HER2:V2}$ affibody molecules were site-specifically labelled with ^{188}Re using freeze-dried labelling kits containing 5 mg of sodium α-D-gluconate, 100 μg of disodium EDTA, and 1 mg of tin(II) chloride dihydrate. After reconstitution, labeling was performed at pH 4.2 and 90 °C for 1h. Ascorbic acid and BSA (bovine serum albumin) are introduced as antioxidants (see Supplemental data).

To evaluate serum stability, freshly labelled ^{188}Re-$Z_{HER2:V2}$ (10 μL) was diluted in a serum sample (200 μL) to a concentration similar to the concentration in blood at the moment of injection, and incubated for 1h at 37^{o}C. The mixture was analyzed using radio SDS-PAGE. A sample of perrhenate was used as reference. The analysis was performed in duplicates.

In Vitro Evaluation

The specificity of binding and cellular processing of ^{188}Re-$Z_{HER2:V2}$ by SKOV-3 cells were evaluated as described in (*15*). Affinity of ^{188}Re-$Z_{HER2:V2}$ binding to SKOV-3 was measured at 4^{o}C using LigandTracer with two concentrations of 49 pM and 98 pM (for details of *in vitro* experiments see Supplement data).

In Vivo Studies

The animal experiments were planned and performed in accordance with national legislation on laboratory animals' protection. The animal study was approved by the local Ethics Committee for Animal Research in Uppsala.

SKOV-3 cells (10^7 cells per mouse) were implanted on the right hind leg of female NMRI nu/nu mice. An average animal weight was 27±2 g, and the average tumor weight was 0.8±0.2 g at the start of experiment. Six groups of mice (n=4) were injected intravenously with ^{188}Re-$Z_{HER2:V2}$ in 100 µL PBS. The injected radioactivity was 53 kBq/mouse for six groups. The injected protein dose was adjusted to 1 µg/mouse by adding non-labelled $Z_{HER2:V2}$. The animals were euthanized at 20 min, 1, 4, 8, 24 and 48 h p.i. One group was injected with 140 kBq/mouse and euthanized at 48 h p.i. For specificity control, one group (n = 3) was pre-injected with 500 µg of $Z_{HER2:342}$ 45 min before injection of ^{188}Re-$Z_{HER2:V2}$ and euthanized at 4 h p.i. Organs and tissue samples (see **Table 1**), GI tract and the remaining carcass were collected and weighed, and their radioactivity was measured in a NaI(Tl) well counter (PerkinElmer). Biodistribution data were corrected for decay and self-attenuation in samples, and organ uptake values were calculated as %IA/g except for the intestinal content, thyroid and the carcass, which was calculated as %IA per whole sample.

In vivo imaging was performed to obtain a visual confirmation of the biodistribution data. Three SKOV-3 bearing mice were injected with 0.7 MBq (8 µg) of ^{188}Re-$Z_{HER2:V2}$. Two mice were injected 4 h and one mouse 1 h before imaging experiment. Immediately before imaging, mice were sacrificed by cervical dislocation and the bladders were excised. The imaging was performed using an Infinia scintillation camera (GE Healthcare) equipped with a

high-energy general purpose (HEGP) collimator. Static images (30 min) were obtained with a zoom factor of 2 in a 256 x 256 matrix.

Dosimetry

Animal dosimetry. To evaluate feasibility of experimental therapy in mice, absorbed doses to tumors and normal tissues were calculated using the anatomically realistic murine Moby phantom developed by Larsson et al (*27*,*28*) based on the biokinetics results. Absorbed doses per injected activity (Gy/MBq) for ^{188}Re-$Z_{HER2:V2}$ were calculated for three tumor localizations: tumors located in the right hind leg, left hind leg and the left flank respectively.

Human dosimetry. For dosimetry estimations in humans, uptake was extrapolated from animal data according to the percent kg/g method (*29*).

$$(\%IA/organ)_{human} = [(\%IA/g)_{animal} \times (kg_{TBweight})_{animal} \times (g_{organ}/(kg_{TBweight})_{human}]$$

Organ time-activity curves were calculated using organ weights of the 58 kg reference adult female (ICRP publication 23). Residence times were calculated as the area under the curve of bi-exponential fits to the animal organ time-activity curves. Remainder of the body residence time was based on radioactivity in carcass. Red marrow activity concentrations were conservatively assumed to be equal to whole blood concentrations. Absorbed doses were estimated using OLINDA/EXM 1.0. For calculation of absorbed dose to the intestines, either the ICRP 30 GI model was applied, using a fraction of 0.35% of the injected activity (the measured value at 1 h p.i.) entering the small intestine, or residence times calculated as above for small intestine and large intestine were used.

In tumor, SUV was assumed to be identical in humans as in rodents as well, and tumor absorbed doses were calculated assuming deposition of all beta energy within the tumor, neglecting any self- or cross-dose from gamma radiation. Dependence of absorbed dose on tumor volume was assessed using the Olinda/EXM 1.0 sphere model.

RESULTS

Labelling and Stability

The labelling method provided high yield (95.8±1%) with radiocolloid content below 1%. Purification using disposable NAP-5 columns provided radiochemical purity over 99%. Up-scaling experiments demonstrated that specific activity of 17.5 MBq/µg (116 GBq/µmol) can be obtained. ^{188}Re-$Z_{HER2:V2}$ was stable in the formulation containing 6 mM ascorbic acid in PBS with 2% BSA (radiochemical purity of 99±1% during 4 h). In the absence of BSA, radiochemical purity was 94±2% after 4 h.

SDS-PAGE analysis was performed after incubation in murine blood plasma at 37^{o}C for 60 min. The main peak corresponded to the monomeric affibody molecule. No peaks indicating aggregation of affibody molecules or transchelation of the radionuclide to blood proteins were observed. The only other radioactivity peak had a path length equal to the path length of ^{188}Re-perrhenate. This peak contained less than 2% of the total activity at the end of the stability test (**Supp. Fig 1)**.

In Vitro Evaluation

In vitro specificity experiment showed that binding of ^{188}Re-$Z_{HER2:V2}$ to SKOV-3 ovarian carcinoma cells can be reduced from 52±1 to 0.84±0.05 % of added activity ($p < 0.0001$) by pre-saturation of HER2 with non-labelled affibody molecule. This indicates that the binding of ^{188}Re-$Z_{HER2:V2}$ was specific. Affinity of ^{188}Re-$Z_{HER2:V2}$ binding to SKOV3 cell at 4^{o}C was 6.4±0.4 pM (**Supp. Fig 2**).

The cellular retention profile (**Figure 1**) showed a rapid drop of the activity during first hour followed by a slow decline with a biological half-life of 19.6 h. The total cellular retention of

the radioactivity was 34.6±1.3% after 24 h of incubation at 37°C. The amount of internalized radioactivity of ^{188}Re-$Z_{HER2:V2}$ was relatively low, less than 4% of total radioactivity after 24 h.

In Vivo Studies

The results of in vivo specificity test (**Figure 2**) showed that pre-saturation of HER2-receptors in xenografts with a parental $Z_{HER2:342}$ decreased tumor uptake of ^{188}Re-$Z_{HER2:V2}$ 4.5-fold ($p < 0.005$). This demonstrates a saturable character of the tumor accumulation and suggests its HER2-specificity. Small but statistically significant decrease of uptake in liver and increase in kidneys was also detected in this experiment.

Biodistribution of ^{188}Re-$Z_{HER2:V2}$ in tumor bearing mice (**Table 1**) was characterized by rapid clearance of radioactivity from all organs and tissues. Low radioactivity in the content of the gastrointestinal tract (less than 2% of injected activity, data not shown) suggested that hepatobiliary pathway played a minor role in the excretion of ^{188}Re-$Z_{HER2:V2}$ or its radiometabolites. Low radioactivity uptake in organs accumulating free perrhenate, i.e. salivary gland, thyroid and stomach, suggests high stability of ^{188}Re-$Z_{HER2:V2}$ to re-oxidation in vivo. Kidneys demonstrated high initial uptake, which decreased rapidly. At 1 h p.i., the renal uptake was approximately equal to tumor uptake, and 4 h p.i., the tumor uptake was five-fold higher.

The tumor uptake was prominent as early as 20 minutes p.i. and was higher than the uptake in any normal organ except from kidneys. The tumor uptake had a maximum at 1 h p.i. (14±2 %IA/g) followed by decrease with a half-life of 15 h.

Scintillation-camera imaging, performed at 1 and 4 h after injection (**Figure 3**), confirmed the results of the biodistribution experiments. The tumor xenografts were the only sites with

prominent accumulation of radioactivity. Kidneys were visualized at 1 h after injection, but at 4 h p.i. only the HER2-expressing tumor xenografts were clearly visible.

Dosimetry

The evaluation of absorbed doses in mice for ^{188}Re-$Z_{HER2:V2}$ is presented in **Table 2**. The self-doses to the majority of organs and tissues were much smaller than absorbed doses to tumors. However, the size of a mouse body is comparable with the range of the beta-particles emitted by ^{188}Re (about 10 mm). For this reason, the total absorbed doses became much higher due to cross-irradiation. For example, the total absorbed dose to bone marrow was approximately 22% of the total absorbed tumor dose. This means that it was impossible to deliver a therapeutically meaningful absorbed dose to tumors (above 50 Gy) without lethal absorbed dose to the red marrow (around 8 Gy for mice). Performing therapy experiments with ^{188}Re-$Z_{HER2:V2}$ therapy in mice was thus considered unethical under these circumstances and due to dimensional differences between mice and humans and range of beta particles, experiments in small animal murine models will generate irrelevant results.

The results of estimated absorbed dose calculations of ^{188}Re-$Z_{HER2:V2}$ in humans using Olinda/EXM 1.0, are presented in **Table 3**. In brief, tumor SUV was approximately constant after 1 h with a mean value of 3.3. Assuming local deposition of all beta energy, and no self- or cross-dose from gamma photons, this would result in an absorbed dose to tumor of 0.65 mGy/MBq. As shown in **Figure 4**, absorbed doses to tumors with the weight of less than10 g would be slightly lower due to incomplete absorption of beta particles, whilst slightly higher absorbed doses are expected in larger tumors due to self-dose from gamma radiation. Absorbed dose to tumor exceeded absorbed dose to kidney and bone marrow, 3.4-fold and 79-fold, respectively.

DISCUSSION

Radioimmunotherapy of radiosensitive hematological malignancies has proven to be successful, but treatment of more radioresistant solid tumors has so far been inefficient. The main reason is a failure to reach tumor absorbed doses above 50 Gy which are typically required to achieve response at external beam therapy (*7*).

Clinical experience with targeted radionuclide therapy using short peptides, particularly somatostatin analogues, demonstrated that the use of small targeting agents can solve problems of both poor tumor penetration and exposure of bone marrow (*30*). Unfortunately, all small HER2-targeting radiolabelled agents, including antibody fragments, diabodies, DARPins and affibody molecules undergo considerable renal reabsorption (*31*). In the case of residualizing radiometal labels, the renal uptake would be higher than tumour uptake for all these targeting proteins.

Our approach is based on the knowledge concerning cellular processing of affibody molecules. The main hypothesis was that the use of a non-residualizing label would cause rapid clearance from kidneys, where affibody molecules are rapidly internalized, degraded, and their radiocatabolites are excreted from cells. At the same time, processing of affibody molecules bound to HER2-expressing cancer cell is slow, and cellular retention is good even in the case of non-residualizing labels. Our previous structure-property relationship studies have demonstrated that the use of a -GGGC peptide-based chelator yields non-residualizing ^{99m}Tc (22) labels with low accumulation in kidneys. The present study has shown that $Z_{HER2:V2}$ can be efficiently labelled with ^{188}Re. The high-fidelity refolding of affibody molecules in physiological conditions (*32*) permitted their direct rhenium labelling at high temperature with high yields. In fact, ^{188}Re-$Z_{HER2:V2}$ preserved high affinity binding (6.4±0.4 pM) to HER2 expressing cells after labelling at 90^{o}C and pH 4.2. Although an in vitro processing study (**Figure 1**) showed low intracellular retention of radiocatabolites, the overall

retention of radioactivity was reasonable with a biological half-life of 19.5 h. ^{188}Re-$Z_{HER2:V2}$ has shown specific uptake in HER2-expressing xenografts in vivo (**Figure 2**). The biodistribution study confirmed that unbound radioactivity was cleared very quickly from blood, and release of retained radioactivity from kidneys was much more rapid than from tumors (**Table 1**). Area under curve (AUC) for tumor exceeded AUC for blood 47-fold, bone 70-fold, and kidneys 2.8-fold. This suggested that the goal of delivering an efficient absorbed dose to tumors while sparing critical organs might be achievable.

We performed dosimetry calculations for ^{188}Re-$Z_{HER2:V2}$ in mice using the anatomically realistic murine Moby phantom (*27*,*28*). The self-doses were in agreement with AUC data, however that total absorbed dose to bone marrow was much higher than the self-dose. It must be noted, that a high total absorbed dose to bone marrow is a phenomenon associated with the use of mice as an animal model. The maximum range of beta-particles from ^{188}Re is 10.4 mm (*7*), which is comparable with the dimensions of a mouse. For this reason, the cross-dose to bone marrow is much higher in mice than in humans. Delivery of therapeutically meaningful absorbed doses to tumors in mice would be associated with lethal absorbed doses to bone marrow.

Human dosimetry was much different due to the larger dimensions of the human body. Upscaling of murine biodistribution data to human suggests that much lower absorbed doses will be delivered to radiosensitive organs in relation to tumor absorbed doses. A maximum absorbed dose of 2 Gy for bone marrow is generally accepted when planning radionuclide therapy; as such absorbed dose is associated with low risk of developing leukaemia (*33*) and low risk for acute bone marrow toxicity. An absorbed dose of 23 Gy is a commonly used absorbed dose limit for kidneys in peptide receptor radionuclide therapy (*34*). In the case of ^{188}Re-$Z_{HER2:V2}$, an absorbed dose of 23 Gy to the kidneys would correspond to tumor absorbed dose of 79 Gy, whilst an absorbed dose of 2 Gy to bone marrow would correspond to tumor

absorbed dose of 130 Gy. This would permit delivering an absorbed dose well above 50 Gy without exceeding commonly accepted absorbed dose limits to critical organs. It has to be mentioned that upscaling from mice to humans is associated with apparent uncertainties, and a clinical imaging study would be required to obtain more reliable assessment of human dosimetry.

In addition to dosimetry estimations, there are other factors to consider when planning future therapy applications. ^{188}Re is produced via a generator in no-carrier-added form, which provides high specific activity. The short half-life of ^{188}Re enables irradiation of tumors with a high dose rate. Close matching of physical and biological half-lives and generator-mediated production from the long-lived mother nuclide ^{188}W (T½=70 d) permits fractionated therapy. Both the absorbed dose rate during tumor irradiation and treatment fractionation are considered as important radiobiological factors for increasing efficacy of targeted radionuclide therapy (*7*).

One important lesson from this study concerns selection of labelling strategy. It is a common knowledge that selection of radionuclide and chelator influences stability of nuclide attachment to a targeting proteins, and intracellular retention of radioactivity after internalization. Our earlier studies have demonstrated that modification of physicochemical properties of affibody molecules by incorporation of radionuclide-chelator complex modifies also off-target interactions, changing blood clearance rate, predominant excretion pathway and biodistribution (*11*). This can be used for optimizing of targeting properties. We have earlier shown that the ^{186}Re-maGSG-$Z_{HER2:342}$ affibody molecule having an N-terminal mercaptoacetyl-glycyl-seryl-glycyl chelator provided, similarly to ^{188}Re-$Z_{HER2:V2}$, better retention of radioactivity in tumors than in kidneys. However, appreciable hepatobiliary excretion of ^{186}Re-maGSG-$Z_{HER2:342}$ (20% of injected radioactivity was measured in the intestinal content at 4 h p.i.) caused a risk of high absorbed dose to intestines. Through re-

engineering of affibody molecules by modifying of the chelator and its placement to C-terminus, as well as increasing hydrophilicity of N-terminus by amino acid substitution, we suppressed hepatobiliary excretion of ^{188}Re-$Z_{HER2:V2}$ while keeping good tumor retention, low renal uptake and rapid clearance of unbound radioactivity. Thus optimal molecular design, including labelling strategy, may appreciably improve properties of scaffold-protein-based conjugates for radionuclide therapy.

Conclusion:

The affibody molecule, $Z_{HER2:V2}$ can be labelled with ^{188}Re with a high yield with preserved picomolar affinity to HER2. ^{188}Re-$Z_{HER2:V2}$ provides efficient targeting of HER2-expressing xenografts, rapid blood clearance and low uptake in kidneys and bones. Dosimetry calculations in man suggest that ^{188}Re-$Z_{HER2:V2}$ may provide absorbed dose to tumors of more than 70 Gy while keeping absorbed dose to kidneys below 23 Gy and absorbed dose to bone marrow below 2 Gy. Thus, ^{188}Re-$Z_{HER2:V2}$ is a promising targeting agent for radionuclide therapy against HER2-expressing tumors.

ACKNOWLEDGMENTS

This research was supported in part by grants from the Swedish Cancer Society (Cancerfonden), Swedish Research Council (Vetenskapsrådet) and Governmental Funding of Clinical Research within the National Health Service (ALF).

REFERENCES

1. Slamon DJ, Leyland-Jones B, Shak S, et al. Use of chemotherapy plus a monoclonal antibody against HER2 for metastatic breast cancer that overexpresses HER2. *N Engl J Med.* 2001;344:783-792.
2. Bang YJ, Van Cutsem E, Feyereislova A, et al. Trastuzumab in combination with chemotherapy versus chemotherapy alone for treatment of HER2-positive advanced gastric or gastro-oesophageal junction cancer (ToGA): a phase 3, open-label, randomised controlled trial. *Lancet.* 2010;376:687-697.
3. Wu AM, Senter PD. Arming antibodies: prospects and challenges for immunoconjugates. *Nat Biotechnol*. 2005;23:1137-1146.
4. Diéras V, Bachelot T. The success story of trastuzumab emtansine, a targeted therapy in HER2-positive breast cancer. *Target Oncol*. Jul 14, 2013[Epub ahead of print].
5. Sharkey RM, Goldenberg DM. Perspectives on cancer therapy with radiolabeled monoclonal antibodies. *J Nucl Med*. 2005;46(Suppl 1):115S–127S.
6. Kenanova V, Wu AM. Tailoring antibodies for radionuclide delivery. *Expert Opin Drug Deliv*. 2006;3:53-70.
7. Pouget JP, Navarro-Teulon I, Bardiès M, et al. Clinical radioimmunotherapy--the role of radiobiology. *Nat Rev Clin Oncol*. 2011;8:720-734
8. Miao Z, Levi J, Cheng Z. Protein scaffold-based molecular probes for cancer molecular imaging. *Amino Acids.* 2011;41:1037-1047.
9. Nygren PA. Alternative binding proteins: affibody binding proteins developed from a small three-helix bundle scaffold. *FEBS J*. 2008;275:2668-2676.
10. Orlova A, Magnusson M, Eriksson TL, et al. Tumor imaging using a picomolar affinity HER2 binding affibody molecule. *Cancer Res.* 2006;66:4339-4348.

11. Feldwisch J, Tolmachev V. Engineering of affibody molecules for therapy and diagnostics. *Methods Mol Biol.* 2012;899:103-126.
12. Baum RP, Prasad V, Müller D, et al. Molecular imaging of HER2-expressing malignant tumors in breast cancer patients using synthetic 111In- or 68Ga-labeled affibody molecules. *J Nucl Med.* 2010;51:892-897.
13. Sörensen J, Sandberg D, Sandström M, et al. First-in-human molecular imaging of HER2 expression in breast cancer metastases using the 111In-ABY-025 Affibody molecule. *J Nucl Med.* 2014;55:730-735.
14. Altai M, Varasteh Z, Andersson K, Eek A, Boerman O, Orlova A. In vivo and in vitro studies on renal uptake of radiolabeled affibody molecules for imaging of HER2 expression in tumors. *Cancer Biother Radiopharm.* 2013;28:187-195.
15. Wållberg H, Orlova A. Slow internalization of anti-HER2 synthetic affibody monomer 111In-DOTA-ZHER2:342-pep2: implications for development of labeled tracers. *Cancer Biother Radiopharm.* 2008;23:435-442.
16. Tolmachev V, Mume E, Sjöberg S, Frejd FY, Orlova A. Influence of valency and labelling chemistry on in vivo targeting using radioiodinated HER2-binding Affibody molecules. *Eur J Nucl Med Mol Imaging.* 2009;36:692-701.
17. Engfeldt T, Tran T, Orlova A, Widström C, Karlström AE, Tolmachev V. 99mTc-chelator engineering to improve tumour targeting properties of a HER2-specific Affibody molecule. *Eur J Nucl Med Mol Imaging.* 2007;34:1843–1853
18. Tran T, Engfeldt T, Orlova A, et al. (99m)Tc-maEEE-Z(HER2:342), an Affibody molecule-based tracer for the detection of HER2 expression in malignant tumors. *Bioconjug Chem*. 2007;18:1956-1964.

19. Tran TA, Ekblad T, Orlova A, et al. Effects of lysine-containing mercaptoacetyl-based chelators on the biodistribution of 99mTc-labeled anti-HER2 Affibody molecules. *Bioconjug Chem*. 2008;19:2568-2576.
20. Ekblad T, Tran T, Orlova A, et al. Development and preclinical characterisation of 99mTc-labelled Affibody molecules with reduced renal uptake. *Eur J Nucl Med Mol Imaging*. 2008;35:2245-2255.
21. Ahlgren S, Wållberg H, Tran TA, et al. Targeting of HER2-expressing tumors with a site-specifically 99mTc-labeled recombinant affibody molecule, ZHER2:2395, with C-terminally engineered cysteine. *J Nucl Med.* 2009;50:781-789.
22. Wållberg H, Orlova A, Altai M, et al. Molecular design and optimization of 99mTc-labeled recombinant affibody molecules improves their biodistribution and imaging properties. J *Nucl Med.* 2011;52:461-469.
23. Altai M, Wållberg H, Orlova A, et al. Order of amino acids in C-terminal cysteine-containing peptide-based chelators influences cellular processing and biodistribution of 99mTc-labeled recombinant Affibody molecules. *Amino Acids.* 2012;42:1975-1985.
24. Cyr JE, Pearson DA, Wilson DM, et al. Somatostatin receptor-binding peptides suitable for tumor radiotherapy with Re-188 or Re-186. Chemistry and initial biological studies. *J Med Chem*. 2007;50:1354–1364.
25. Orlova A, Tran TA, Ekblad T, Karlström AE, Tolmachev V. (186)Re-maGSG-Z (HER2:342), a potential Affibody conjugate for systemic therapy of HER2-expressing tumours. *Eur J Nucl Med Mol Imaging*. 2010;37:260-269.
26. Wållberg H, Löfdal PÅ , Tschapalda K. Affinity recovery of eight HER2-binding affibody variants using an anti-idiotypic affibody molecule as capture ligand. *Protein Expr Purif*. 2011;76:127–135.

27. Larsson E, Strand SE, Ljungberg M, Jönsson BA. Mouse S-factors based on Monte Carlo simulations in the anatomical realistic Moby phantom for internal dosimetry. *Cancer Biother Radiopharm*. 2007;22:438-442.

28. Larsson E, Ljungberg M, Strand SE, Jönsson BA. Monte Carlo calculations of absorbed doses in tumours using a modified MOBY mouse phantom for pre-clinical dosimetry studies. *Acta Oncol*. 2011;50:973-980.

29. Stabin MG. Fundamentals of Nuclear Medicine Dosimetry. New York, NY: Springer; 2008:83-86.

30. van Essen M, Krenning EP, Kam BL, de Jong M, Valkema R, Kwekkeboom DJ. Peptide-receptor radionuclide therapy for endocrine tumors. *Nat Rev Endocrinol.* 2009;5:382-393.

31. Tolmachev V. Imaging of HER-2 overexpression in tumors for guiding therapy. *Curr Pharm Des*. 2008;14:2999-3019

32. Arora P, OasTG, Myers JK. Fast andfaster: a designed variant of the B domain of protein A folds in 3 microsec. *Protein Sci*. 2004;13:847–853.

33. Forrer F, Krenning EP, Kooij PP, et al. Bone marrow dosimetry in peptide receptor radionuclide therapy with [177Lu-DOTA(0),Tyr(3)]octreotate. *Eur J Nucl Med Mol Imaging*. 2009;36:1138-1146.

34. Kwekkeboom DJ, de Herder WW, van Eijck CH, et al. Peptide receptor radionuclide therapy in patients with gastroenteropancreatic neuroendocrine tumors. *Semin Nucl Med*. 2010;40:78-88.

Table 1. Biodistribution of ^{188}Re-$Z_{HER2:V2}$ in NMRI nu/nu mice bearing HER2-expressing SKOV-3 xenografts.

	Uptake *					
Organ	**20 min.**	**1h**	**4h**	**8h**	**24h**	**48h**
Blood	3.0±0.3	1.4±0.1	0.3±0.1	0.05±0.02	0.02±0.01	0.006±0.003
Heart	1.4±0.3	0.6±0.1	0.11±0.02	0.05±0.01	0.02±0.01	NM
Lung	3.4±0.2	1.7±0.2	0.28±0.05	0.08±0.03	0.03±0.01	NM
Salivary gland	1.6±0.5	1.1±0.3	0.2±0.1	0.06±0.03	0.02±0.01	NM
Thyroid*	0.07±0.02	0.04±0.02	0.01±0.001	0.01±0.004	0.002±0.001	NM
Liver	3.4±0.3	2.2±0.2	0.51±0.09	0.26±0.06	0.12±0.03	0.06±0.016
Spleen	1.5±0.2	0.87±0.06	0.16±0.02	0.08±0.01	0.03±0.01	NM
Pancreas	0.8±0.2	0.4±0.1	0.08±0.03	0.030±0.003	0.01±0.01	NM
Stomach	2.0±0.08	1.3±0.23	0.3±0.1	0.08±0.01	0.08±0.07	NM
Small intestine	1.4±0.1	0.9±0.2	0.16±0.08	0.08±0.07	0.04±0.03	NM
Large intestine	1.9±0.08	1.2±0.6	0.19±0.05	0.3±0.3	0.04±0.01	0.02±0.004
Kidney	47±2	18±3	2.1±0.2	1.0±0.2	0.51±0.08	0.30±0.12
Tumor	8.7±0.9	14±2	12±2	8.0±0.6	5±2	1.8±0.5
Skin	2.4±0.4	1.4±0.1	0.6±0.5	0.10±0.02	0.04±0.02	0.02±0.005
Muscle	0.6±0.1	0.28±0.03	0.06±0.03	0.02±0.01	0.02±0.01	NM
Bone	1.0±0.1	0.6±0.1	0.12±0.01	0.05±0.02	0.04±0.02	NM
Brain	0.08±0.02	0.05±0.01	0.020±0.003	0.01±0.001	0.01±0.002	NM
Carcass**	23±2	14±4	2±1	1.1±0.9	0.35±0.09	0.19±0.04

*The uptake is expressed as %IA/g and presented as an average value from 4 animals±standard deviation. Data are corrected for decay and self-attenuation in samples.
*data for thyroid and carcass are presented as % of injected activity per whole sample.
NM = not measurable, below detection limit.

Table 2. Calculated absorbed dose in (Gy/MBq) for ^{188}Re-$Z_{HER2:V2}$ in mice using murine Moby phantom.

Organ	Self-dose	Total absorbed dose
Blood	0.008	0.099
Heart	0.003	0.094
Lung	0.019	0.14
Salivary gland	0.0062	0.11
Thyroid	0.00022	0.13
Liver	0.027	0.079
Spleen	0.0068	0.072
Pancreas	0.0024	0.075
Stomach	0.014	0.061
Small intestine	0.0058	0.076
Large intestine	0.0051	0.11
Kidney	0.17	0.23
Skin	0.0038	0.081
Bone	0.0019	0.10
Brain	0.00073	0.026
Carcass	0.16	0.16
Tumor 1*	0.40	0.43
Tumor 2*	0.40	0.43
Tumor 3*	0.40	0.44
Bone Marrow	0.0029	0.096

Tumor 1, 2 and 3 stands for tumors located in the right hind leg, left hind leg and the left flank respectively.

Table 3. Calculated absorbed dose in (mGy/MBq) for ^{188}Re-$Z_{HER2:V2}$ in humans using Olinda/EXM 1.0.

Organ	Absorbed dose ^{188}Re-$Z_{HER2:V2}$
Adrenals	0.007
Brain	0.002
Breasts	0.006
Gallbladder Wall	0.007
LLI Wall	0.022 (0.046*)
Small Intestine	0.018 (0.014*)
Stomach Wall	0.007
ULI Wall	0.034
Heart Wall	0.006
Kidneys	0.189
Liver	0.029
Lungs	0.011
Muscle	0.006
Ovaries	0.007
Pancreas	0.006
Red Marrow	0.010
Osteogenic Cells	0.020
Skin	0.006
Spleen	0.009
Thymus	0.006
Thyroid	0.001
Urinary Bladder Wall	0.006
Uterus	0.007
Total Body	0.009
Tumor	0.65

*Using GI tract model assuming 0.35% of the injected dose entering small intestine.

FIGURES

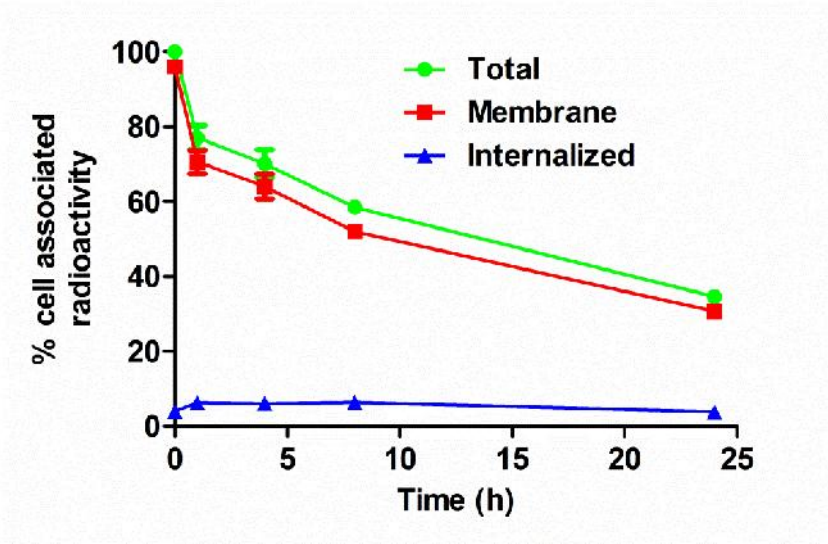

Figure 1. Cell-associated radioactivity as function of time after interrupted incubation of SKOV-3 cells with ^{188}Re-$Z_{HER2:V2}$. Data are presented as average value from 3 cell dishes ± SD. Error bars might not be seen because they are smaller than point symbols.

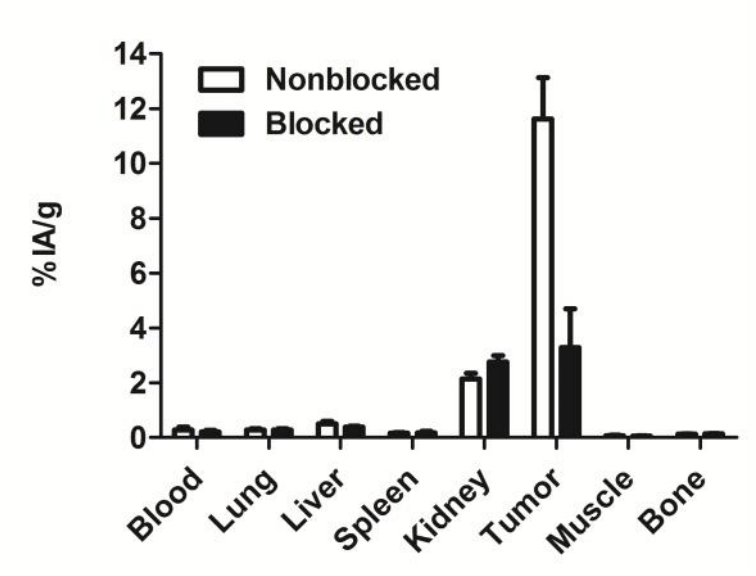

Figure 2. In vivo binding specificity of ^{188}Re-$Z_{HER2:V2}$ in mice bearing ovarian cancer SKOV-3 xenografts at 4 h after injection. The blocked group was subcutaneously pre-injected with excess amount of non-labelled $Z_{HER2:342}$. Results are presented as percentage of injected activity per gram of tissue (%IA/g).

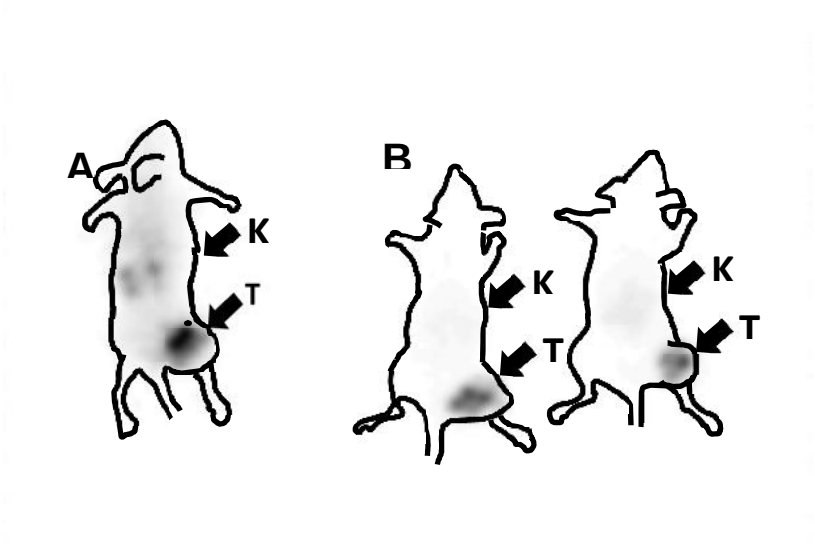

Figure 3. Imaging of HER2 expression in SKOV-3 ovarian cancer xenografts (high HER2 expression) in NMRI nu/nu mice using ^{188}Re-$Z_{HER2:V2}$. Planar scintillation-camera images were acquired at 1 h (A) and 4 h (B) after injection. Arrows point to tumors (T) and kidneys (K).

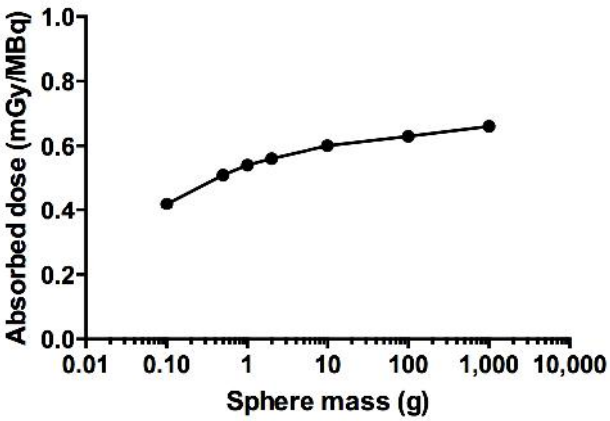

Figure 4. Tumor absorbed dose versus mass for ^{188}Re-$Z_{HER2:V2}$.

SUPPLEMENTAL DATA

Labelling and stability

^{188}Re was obtained as perrhenate by elution of a ^{188}W/^{188}Re generator (29.6 GBq) with 0.9% sodium chloride (Polatom). Elution efficiency was 90%, when 4 ml of eluent was used.

For animal studies, the content of one freeze-dried kit was dissolved in100 µL 1.25 M sodium acetate, pH 4.2, and added to 100 µg of freeze-dried $Z_{HER2:V2}$. To the reaction mixture, 14-100 µL of ^{188}Re-containing generator eluate was added under argon gas. An equivalent of 220 µg ascorbic acid (2 mg/mL in 1.25 M sodium acetate buffer, pH 4.2) was added to the reaction vial. The mixture was incubated at 90°C for 60 min and then cooled at room temperature for 5 min. Thereafter, the total amount of ascorbic acid in the reaction vial is adjusted to 1 mg with a 5 mg/mL ascorbic acid solution in PBS (phosphate buffered saline) containing 2% BSA (bovine serum albumin). ^{188}Re-$Z_{HER2:V2}$ was purified using disposable NAP-5 columns (GE Healthcare) pre-equilibrated and eluted with PBS containing 2% BSA. The final solution was diluted with an extra 100 µL PBS containing 2% BSA and 500 µg ascorbic acid to a final volume of 1 mL.

In up-scaling experiments, the content of a freeze-dried labelling kit vial (4 mg tin(II) chloride dihydrate, 400 µg disodium EDTA and 20 mg of sodium α-D-gluconate) was reconstituted in 400 µL 1.25 M sodium acetate, pH 4.2, containing 5mg/ml acid, and votrexed. The content of the vial was transferred to another vial containing 400 µg freeze-dried $Z_{HER2:V2}$ and vortexed. To this mixture, a 1mL (~7 GBq) of ^{188}Re-containing generator eluate was added, and the labeling mixture was votrexed carefully and incubated at 95^{o}C for 60 min. Further processing was performed as described above.

For measurement of the labelling yield and radiochemical purity, samples of ^{188}Re-$Z_{HER2:V2}$ were analyzed using ITLC SG strips eluted with PBS. For measurement of reduced

hydrolyzed rhenium colloid levels, a pyridine:acetic acid:water (5:3:1.5) mobile phase was used. The ITLC analysis was cross-calibrated by SDS-PAGE (Novex 4-12% Bis-Tris Gel, MES buffer, 200 V constant).

To estimate the shelf-life, the purity of ^{188}Re-$Z_{HER2:V2}$ was measured at 1, 2 and 4h after purification using ITLC in duplicates.

In vitro evaluation

In vitro specificity test was performed using SKOV-3 cells. Briefly, a solution of ^{188}Re-$Z_{HER2:V2}$ (0.015 ng protein per dish, 2 nM) was added to six Petri dishes (ca. 10^6 cells in each). For blocking, an excess of non-labeled recombinant $Z_{HER2:342}$ (7.4 µg) was added 10 min. before ^{188}Re-$Z_{HER2:V2}$ to saturate the receptors. The cells were incubated during one hour in a humidified incubator at 37°C. Thereafter, the media was collected, the cells were detached by trypsin-EDTA solution, and the radioactivity in cells and media was measured to calculate a percentage of cell-bound radioactivity.

For cellular processing SKOV-3 cells (1×10^6 cells/dish) were incubated with 2 nM solution of labeled affibody at 4°C. After 1 h incubation, the medium with the labeled compound was removed and cells were washed three times with ice-cold serum-free medium. One mL of complete media was added to each dish and cells were further incubated at 37°C in an atmosphere containing 5% CO_2. At designated time points (0 h, 1 h, 4 h, 8 h and 24 h), a group of three dishes was removed from the incubator, the media was collected and cells were washed three times with ice-cold serum-free medium. Thereafter, cells were treated with 0.5 mL 0.2 M glycine buffer, pH 2, containing 4 M urea, for 5 min on ice. The acidic solution was collected and cells were additionally washed with 0.5 mL glycine buffer. The acidic fractions were pooled. The cells were then incubated with 0.5 mL 1 M NaOH at 37°C for 30 min. The cell debris was collected, and the dishes were additionally washed with 0.5 mL of

NaOH solution. The alkaline solutions were pooled. The radioactivity in the acidic solution was considered as membrane bound, and in the alkaline fractions as internalized.

Affinity determination using LigandTracer

SKOV-3 cells were seeded on a local area of a cell culture dish (NunclonTM, Size 100620, NUNC A/S, Roskilde, Denmark), as described previously (1). The binding of ^{188}Re-labeled anti-HER2 affibody molecules to living cells was monitored in real-time at 4^{o}C using LigandTracer Yellow, using established methods described in Björkelund *et al*. In brief, the LigandTracer records the real-time kinetics of binding and dissociation of radiolabeled tracer in living cells. By using the TraceDrawer software, which allows the calculation of both association and dissociation rate, it becomes possible to determine the affinity of radiolabeled conjugate (1). In order to cover the concentration span needed for proper affinity estimation, two increasing concentrations of 49 pM and 98 pM (selected based on previous K_D values obtained using Biacore) of each variant were added in each affinity assay **Supp. Fig 2**.

References

(1) Björkelund, H.; Gedda, L.; Barta, P.; Malmqvist, M.; Andersson, K. Gefitinib induces epidermal growth factor receptor dimers which alters the interaction characteristics with ^{125}I-EGF. *PLoS One.* **2011**, 6, e24739

Suppl. Figure 1. SDS–PAGE analysis of the stability of ^{188}Re-$Z_{HER2:V2}$ in murine serum. 1. incubated in murine serum at 37°C for 1 h; 2. $^{188}ReO_4^-$ used as a marker for low-molecular-weight compounds. Signal, measured as digital light units, is in proportion to radioactivity in given point of lane in SDS-PAGE gel. DLU=digital light units.

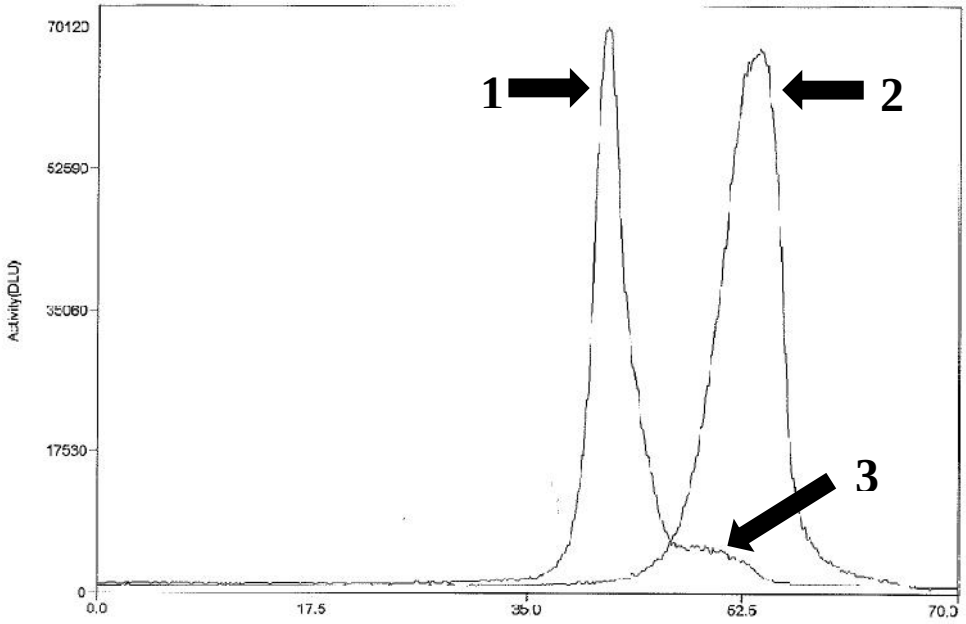

Suppl. Figure 2. LigandTracer sensorgram of interaction of ^{188}Re-$Z_{HER2:V2}$ with HER2-expressing SKOV-3 cells. Concentrations of ^{188}Re-$Z_{HER2:V2}$ were 49 pM and 98 pM.